

# Double aperture focusing transducer for controlling microparticle motions in trapezoidal microchannels with surface acoustic waves

Ming K. Tan, Ricky Tjeung, Hannah Ervin, Leslie Y. Yeo, and James Friend<sup>a)</sup>

*Micro/Nanophysics Research Laboratory, Monash University, Clayton, Victoria 3800, Australia*

(Received 1 August 2009; accepted 4 September 2009; published online 28 September 2009)

We present a method for controlling the motion of microparticles suspended in an aqueous solution, which fills in a microchannel fabricated into a piezoelectric substrate, using propagating surface acoustic waves. The cross-sectional shape of this microchannel is trapezoidal, preventing the formation of acoustic standing waves across the channel width and therefore allowing the steering of microparticles. The induced acoustic streaming transports these particles to eliminate the use of external pumps for fluid actuation. © 2009 American Institute of Physics. [doi:10.1063/1.3238313]

By using acoustic forces, the motions of suspended microparticles in a fluid that flows in a microchannel may be controlled and therefore facilitate their manipulation in microfluidics applications. One of the advantages of using acoustic waves to control the particle motion in microchannels is that the size of the device can be reduced by increasing the frequency ( $f$ ), a characteristic that is suitable for the development of portable flow cytometers for sorting of live cells—that is, if it is possible to increase the frequency enough to deliver acoustic radiation with wavelengths commensurate with the dimensions of microfluidics devices. Jinjie *et al.*<sup>1</sup> and Kapishnikov *et al.*<sup>2</sup> demonstrated that this is indeed possible by forming standing acoustic waves across a microchannel to collect particles in an aqueous suspension along the acoustic pressure nodal lines. Current cytometers, though very expensive, are ubiquitous in analyzing up to many hundreds of thousands of particles by sorting such particles based on some specific characteristic—live versus dead cells, for example—and are essential to the clinical and research-driven diagnosis of many diseases and disorders.

When finite amplitude (high intensity) acoustic waves propagate in a fluid particle suspension, acoustic radiation force and acoustic streaming (Stokesian) drag dominate other forces on the particles.<sup>3,4</sup> High intensity, periodic acoustic waves propagating in the fluid induce *acoustic streaming*:<sup>5,6</sup> the time-averaged values of acoustic parameters, including the sound pressure and acoustic particle velocity ( $u_1$ ), are nonzero. For acoustic fields, fluid motion occurs in a time scale of  $\mathcal{T}_A \sim \mathcal{O}(f^{-1})$  s, whereas for acoustic streaming, fluid motion occurs in a typical hydrodynamic time scale of  $\mathcal{T}_s \sim \mathcal{O}[(\alpha u_1)^{-1}]$  s, where  $\alpha$  is the sound absorption coefficient. In the experiments of Kapishnikov *et al.*,<sup>2</sup> the acoustic radiation force is only used for controlling the particle motion and the acoustic streaming is insignificant because the intensity of the radiation is low. Flow along these microchannels is driven by an external pump. In this work, we experimentally demonstrate a method to utilize both the acoustic radiation force and acoustic streaming force to not only control the particle motion but also to pump the fluid in the channel. A significant difference from the method of Jinjie *et al.*<sup>1</sup> is that this method relies on propagating waves rather than standing waves. Figure 1 illustrates the concept.

Surface acoustic waves (SAWs) are generated on a piezoelectric substrate by applying a high frequency electrical sinusoidal signal to an interdigital transducer (IDT). A substantial amount of SAW energy is transmitted from the substrate into the adjacent fluid, generating compressional acoustic waves and SAW streaming in the fluid. The motion of particles suspended in an aqueous solution may be controlled using SAW.<sup>7–10</sup> Shilton *et al.*<sup>8</sup> demonstrated the effectiveness of induced SAW streaming for concentrating particles in microdrops and suggested that IDTs with curved electrodes are most effective in this application. This is due to the focusing of the SAW radiation and commensurate increase in its intensity due to the curved electrodes. Tan *et al.*<sup>11</sup> further exploited high intensity focused SAWs to generate slender microjets.

The effect of SAW on particles in microchannels has also been investigated,<sup>9</sup> in which the authors demonstrate that induced SAW streaming is capable of transporting particles at a velocity on the order of 10 mm/s. This work is essentially built on those reported results to investigate the effect of high intensity, propagating focused SAWs on particles suspended in an aqueous solution that completely fills the microchannel illustrated in Fig. 1(b). These waves are generated using a focusing transducer divided into two halves and known as a double aperture transducer. Such transducers are able to generate SAW that is more intense on one side of the channel by exciting one half of the transducer, thereby generating an unbalanced acoustic pressure force on the particles across the width of the channel. This net acoustic radiation force pushes the particles away from the wall experiencing a higher SAW intensity.

In the past, double aperture IDTs have been investigated for use as filters in wireless communication devices or in

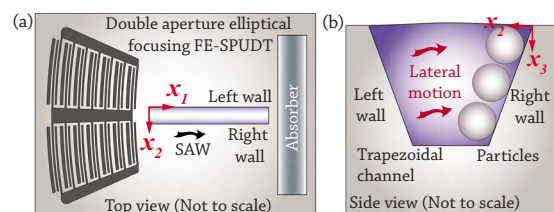


FIG. 1. (Color online) Illustration of the fluid pumping and particle manipulation concept. (a) A channel is fabricated on 128-YX-LN substrate fabricated with a double aperture elliptical focusing FE-SPUDT. An absorber is used to minimize radiation reflection. (b) The trapezoidal cross section channel prevents the formation of standing waves across the channel.

<sup>a)</sup>Electronic mail: james.friend@eng.monash.edu.au.

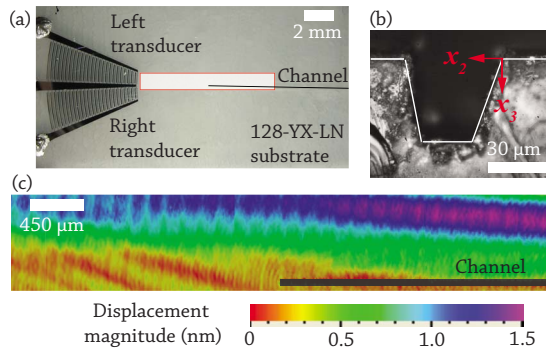


FIG. 2. (Color online) (a) shows a 30.15 MHz elliptical focusing FE-SPUDT with an approximate eccentricity of 0.616, fabricated on a 128-YX-LN substrate. The channel was located along the central line of the transducer. The (b) image shows the cross-sectional shape of the trapezoidal channel. (c) The measured surface displacement magnitude for the area highlighted in (a). Due to the low eccentricity of this elliptical transducer, the focal point of these high intensity SAWs is located close to the middle of the channel (along  $x_1$  direction).

radio-frequency (rf) identification tag systems.<sup>12</sup> However, to the best of our knowledge, their potential for use in microfluidic applications has been overlooked. Figure 2(a) shows a 30.15 MHz double aperture floating-electrode single-phase unidirectional transducer (FE-SPUDT). This transducer was fabricated on a 500  $\mu\text{m}$  thick 128° rotated  $Y$ -cut  $X$ -propagating lithium niobate (128-YX-LN) substrate. The SPUDT transmits acoustic energy predominantly in the forward direction.<sup>13</sup> One significant difference between the device fabricated in this work and those typically designed for rf filtering is the *elliptical* shape of our transducers. As discussed previously, the focusing effect of an elliptical transducer is desirable in this situation, but it is not particularly useful for rf filtering applications. Figure 2(c) shows the SAW propagation pattern measured using scanning laser Doppler vibrometry (Polytec PI MSA-400, Waldbrunn, Germany) for the 30.15 MHz double aperture FE-SPUDT on the highlighted area in Fig. 2(a).

The microchannel used in this work was specially designed to avoid the formation of standing waves in the channel. Microchannels with rectangular cross sections have been studied;<sup>9</sup> though they are easier to fabricate, they also create strong transverse acoustic standing waves (along the  $x_2$  direction, see Fig. 1) as a result of the superposition of waves radiated from the parallel—left and right—walls of the channel. Such standing waves are so easily generated that they effectively prevent the transverse transport of particles using even our double aperture transducer. To avoid this problem, a trapezoidal cross section was chosen in order to prevent the formation of such standing waves. The channel was fabricated using a 248 nm excimer laser (MiniFAB, Scoresby, Australia). In order to have a trapezoidal cross section, a T-shaped mask was used during laser machining. The dimensions of the channel are approximately 1 cm long (along  $x_1$  axis), 45  $\mu\text{m}$  deep (along  $x_3$  axis), 55  $\mu\text{m}$  wide at the top, and 30  $\mu\text{m}$  wide at the bottom (along  $x_2$  axis), as illustrated in Figs. 1 and 2(b). The left wall is slanted at an angle of approximately 10° and the right wall at 20°, measured from the vertical plane. Interestingly, this concept is similar to the design of studios for orchestra recording where (in addition to the use of building materials of high acoustic absorption) the walls surrounding the room are nonparallel to prevent the formation of standing acoustic waves in the room. More spe-

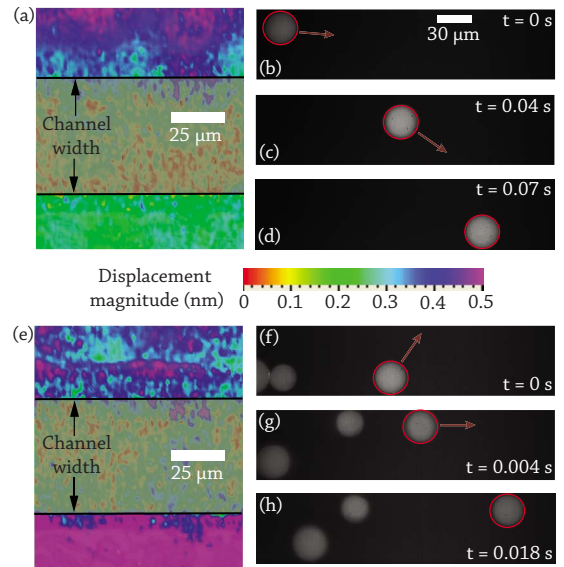


FIG. 3. (Color online) The magnitude of surface displacement perpendicular to the LN substrate surface when the SAW is generated from the (a) left, and (e) right transducer [the left and right transducers are labeled in Fig. 2(a)]. For the same section of the channel, (b)–(d) and (f)–(h) show a 30  $\mu\text{m}$  particle being pushed away from the high vibration magnitude wall to the low vibration wall when the excitation is on the left and right transducer, respectively. The arrow points in the direction the particles are moving. The videos were recorded at 500 frames per second and the measured electrical input power to the transducer was approximately 3 W.

cifically, if the shortest distance between any two parallel walls in the room is  $\mathcal{D}_{\parallel} \approx 5$  m, and compare this to the sound wavelength  $\lambda_f$  of a 200 Hz tone ( $\lambda_f \approx 1.7$  m), we find that  $\mathcal{D}_{\parallel} \sim 3\lambda_f$ . Similarly, the channel used in this work is  $\mathcal{W}_{\text{ch}} \approx 55$   $\mu\text{m}$  wide and the wavelength of a 30 MHz SAW in water at room temperature is  $\lambda_f \approx 48$   $\mu\text{m}$ , therefore,  $\mathcal{W}_{\text{ch}} \sim \lambda_f$ . A strong similarity exists in this regard between these two systems despite the wildly different scale.

In the experiment, homogeneous fluorescent polystyrene particles suspended in an aqueous solution were dispensed into the channel using a syringe. The motion of the particles were observed through a stereomicroscope (Olympus BXFM, Tokyo, Japan) under a mercury light source (EXFO X-Cite 120W short arc lamp, Olympus, Tokyo, Japan) and then recorded via a high speed video camera (MotionBLITZ HSC-kit, Mikrotron, Germany). The IDT used in this experiment has a resonance frequency of 30.15 MHz. Six different particle sizes were used in the experiment: 0.025, 0.5, 1, 5, 9.9, and 31  $\mu\text{m}$  (Duke Scientific, Victoria, Australia).

Figures 3(a) and 3(e) show the measured surface displacement magnitude when the left (a) and right (e) aperture of the transducer is excited with a total input power of approximately 3 W. By keeping the electrical input power at the same level, the measured results show that the left transducer is weaker than the right transducer. We suspect this is due to slight misalignment of the transducers in the  $x_1$  axis of

TABLE I. The estimated orders of magnitude for the forces exerted on a particle of diameter  $\phi_p$ .

Forces	$\phi_p = 30$ $\mu\text{m}$ (N)	$\phi_p = 1$ $\mu\text{m}$ (N)	$\phi_p = 25$ nm (N)
$F_R$	$10^{-10}$	$10^{-12}$	$10^{-30}$
$F_D$	$10^{-11}$	$10^{-12}$	$10^{-14}$

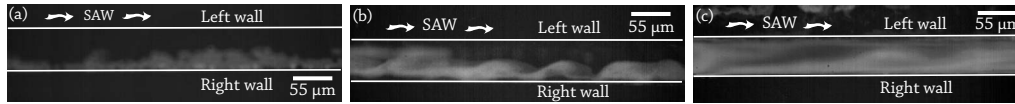


FIG. 4. Experimental images of the particle streaklines for (a) 10, (b) 1, and (c) 0.5  $\mu\text{m}$  polystyrene microspheres in the trapezoidal cross section channel driven by the left transducer [see Fig. 2(a) for the channel cross section and left transducer]. As the particles' size is reduced, the particle suspension becomes more evenly distributed. The measured electric input power to the transducer was approximately 5 W.

the 128-YX-LN substrate compared to the location of the laser-cut channel. Nonetheless, the 30  $\mu\text{m}$  particle was observed to move from the high vibration magnitude channel wall to the opposite low vibration magnitude wall when the device was excited; the split electrode IDT configuration permits this to be done. See Figs. 3(b)–3(d) for the excitation of the left transducer and Figs. 3(f)–3(h) for the right transducer.

We use the expressions derived by King<sup>14</sup> to estimate the acoustic radiation force on a small ( $\omega R_p/c_0 \ll 1$ ) or large ( $\omega R_p/c_0 = 1$ ) rigid sphere due to a plane traveling acoustic wave in the surrounding fluid,

$$F_R \sim 2\pi\rho_0|A|^2 \left(\frac{\omega}{c_0}R_p\right)^6 \frac{1 + \frac{2}{9}[1 - (\rho_0/\rho_p)]^2}{(2 + \rho_0/\rho_p)^2} \quad (1)$$

and

$$F_R \sim \pi\rho_0|A|^2 \frac{1}{89} \frac{95 - 48(\rho_0/\rho_p) + 36(\rho_0/\rho_p)^2}{5 + 6(\rho_0/\rho_p) + 2(\rho_0/\rho_p)^2}, \quad (2)$$

respectively. The  $\rho_0$  is the density of water,  $\rho_p$  is the density of the particle,  $A$  is the complex amplitude of the velocity potential of the incident wave,  $\omega$  is the angular frequency,  $c_0$  is the speed of sound in water, and  $R_p$  is the radius of the particle. The density of the polystyrene microsphere is approximately 1050  $\text{kg}/\text{m}^3$  and therefore we assume here that  $\rho_0/\rho_p \approx 1$ . For the 30 MHz driving frequency, the 30  $\mu\text{m}$  particles are “large particles” according to our definition, while the other sizes of the particles are all “small.” We note here that for a 30.15 MHz SAW, the wavelength in the LN substrate is approximately  $\lambda_{\text{SAW}} \approx 132 \mu\text{m}$  and approximately  $\lambda_f \approx 49 \mu\text{m}$  in the fluid. The acoustic streaming drag force may be estimated from  $F_D \sim \pi\mu u_{\text{dc}} R_p$ , where  $\mu$  is the fluid viscosity and  $u_{\text{dc}}$  is the streaming velocity.

Table I shows the estimated order of magnitude of the acoustic radiation force and acoustic streaming drag on a microparticle, depending on its size. The magnitude of streaming velocity is assumed to be approximately 1 mm/s and the first-order acoustic particle velocity is approximately 0.1 m/s. We note here that the measured streaming velocity in this work is found to be smaller than a previously reported velocity.<sup>9</sup> This is due to the fact that the SAW radiation is intense on only one side of the channel wall (a configuration identical to a single acoustic radiator), therefore the effectiveness of the device in pumping the fluid is reduced [see Fig. 2(c)]. Based on the estimated order of magnitude listed in Table I, we found that the lateral motion of the 30  $\mu\text{m}$  particle [see Figs. 3(b)–3(d) and 3(f)–3(h)] is driven by the strong acoustic radiation force. For the 1  $\mu\text{m}$  particle, the acoustic radiation force is the same order of magnitude as the acoustic streaming force, suggesting that while the particle is being pushed away from the high vibration amplitude channel wall to the opposite channel wall, acoustic streaming

drags the particles to follow the fluid flow [see Fig. 4(b)]. By reducing the particle size, the acoustic radiation force falls significantly. Eventually, the streaming drag dominates and thus leads to the disappearance of the lateral motion of the particles [see Fig. 4(c)]. This essentially means the smaller particles are subjected to stronger streaming drag and thus are less likely to be pushed to one side of the channel wall. The results for the 10, 1, and 0.5  $\mu\text{m}$  particles, shown in Figs. 4(a)–4(c), clearly demonstrate this phenomenon. The vortical flow observed in Figs. 4(b) and 4(c) has been reported previously.<sup>9</sup>

Using double aperture focusing transducers to generate nonuniform acoustic waves along the microchannels walls together with a trapezoidally cross-sectioned microchannel to prevent the formation of standing acoustic waves within it allows one to laterally position and axially transport suspended particles. Such an ability is useful for a wide variety of applications, particularly in cell cytometry. The main advantage of using propagating acoustic waves is the ability to transport particle suspensions along the channel without having to use external pumps. Furthermore, using well-known analytical expressions, we have examined the effectiveness of particle collection based on the size of the particles at a fixed operating frequency of the device, finding that larger particles are more sensitive to the laterally imposed acoustic radiation forces than smaller particles. This information is crucial to determine and select the appropriate operating frequency of the SAW device, in which the size of the particle (to be controlled) is a critical factor, not to mention the potential for sorting particles laterally across the channel based on their size.

<sup>1</sup>J. Shi, X. Mao, D. Ahmed, A. Colletti, and T. J. Huang, *Lab Chip* **8**, 221 (2008).

<sup>2</sup>S. Kapishnikov, V. Kantsler, and V. Steinberg, *J. Stat. Mech.: Theory Exp.* **2006**, P01012 (2006).

<sup>3</sup>Q. Qi and G. J. Brereton, *IEEE Trans. Ultrason. Ferroelectr. Freq. Control* **4**, 619 (1995).

<sup>4</sup>M. K. Tan, J. R. Friend, and L. Y. Yeo, *Appl. Phys. Lett.* **91**, 224101 (2007).

<sup>5</sup>W. L. Nyborg, in *Acoustic Streaming*, edited by W. P. Mason and R. N. Thurston, (Academic, New York, 1965), Chap. 11, pp. 265–329.

<sup>6</sup>T. Uchida, T. Suzuki, and S. Shiokawa, *Ultrason. Symp. Proc.* **2**, 1081 (1995).

<sup>7</sup>M. Takeuchi and K. Yamanouchi, *Jpn. J. Appl. Phys., Part 1* **33**, 3045 (1994).

<sup>8</sup>R. Shilton, M. K. Tan, L. Y. Yeo, and J. R. Friend, *J. Appl. Phys.* **104**, 014910 (2008).

<sup>9</sup>M. K. Tan, L. Y. Yeo, and J. R. Friend, *EPL* **87**, 47003 (2009).

<sup>10</sup>M. K. Tan, J. R. Friend, and L. Y. Yeo, *Lab Chip* **7**, 618 (2007).

<sup>11</sup>M. K. Tan, J. R. Friend, and L. Y. Yeo, *Phys. Rev. Lett.* **103**, 024501 (2009).

<sup>12</sup>S. Lehtonen, V. P. Plessky, C. S. Hartmann, and M. M. Salomaa, *IEEE Trans. Ultrason. Ferroelectr. Freq. Control* **51**, 1697 (2004).

<sup>13</sup>C. S. Hartmann and B. P. Abbott, *Proc. IEEE* **1**, 79 (1989).

<sup>14</sup>L. V. King, *Proc. R. Soc. London, Ser. A* **147**, 212 (1934).